Journal of Inorganic and General Chemistry
ZAAC
Zeitschrift für anorganische und allgemeine Chemie
www.zaac.wiley-vch.de
RESEARCH ARTICLE
DOI: 10.1002/zaac.202200026

Structural changes in Ba-compounds of different hardness induced by high-energy ball milling – evidenced by ^{137}Ba NMR and X-ray powder diffraction

Steffen Zänker,[a, b] Gudrun Scholz,[b] Julien Marquardt,[a] and Franziska Emmerling*[a, b]

Dedicated to Professor Caroline Röhr on the occasion of her 60th birthday.

Changes in the global bulk and local structures, of three different barium compounds ($BaZrO_3$, BaF_2, and BaFCl),were induced by mechanical milling and followed using X-ray powder diffraction (PXRD), subsequent microstructure analysis, and ^{137}Ba solid state NMR spectroscopy. Harder materials like $BaZrO_3$ experience significantly higher structural changes upon milling than softer materials like BaF_2. Moreover, soft materials with layered structures, like BaFCl, show a pronounced structural change during the milling process. By combining PXRD and solid state NMR, detailed information on the changes to the global and local structures were obtained, which are of interest for mechanochemical synthesis, mechanically treated catalysts or ionic conductors.

Introduction

Solid state mechanochemistry is an attractive, eco-friendly, and efficient alternative to solvent-based, classical synthesis routes.[1–3] Compared to solution-based protocols, mechanochemical syntheses are highly reproducible and can minimize or even avoid the use of solvents. For many of these syntheses, it has been shown that a scale-up is possible.[4] The use of mechanochemistry, for the preparation of inorganic materials, has a long tradition,[1,5] whereas its use in crystal engineering,[6] organic chemistry,[3,7] the formation of metal-organic frameworks, and coordination polymers[8] are newer research topics in mechanochemistry. New compounds with high crystallinity can also be built up during mechanochemical reactions, with their crystallinity being affected during the milling process.[7,9] To highlight the potential of mechanochemistry, IUPAC recently identified mechanochemistry as a technology with the potential to change the world.[10] To unleash the full potential of mechanochemistry and enhance its use in academia and industry, mechanochemical transformations and key steps during the mechanochemical process need to be understood.

During ball milling, a reduction of particle and crystallite sizes, down to the nanometer range, and amorphization of the starting materials can be observed.[11] Nanocrystalline materials often contain particles with a crystalline core surrounded by a stable disordered layer.[12] Furthermore, the morphology of mechanochemically produced samples and samples obtained from solution may differ.[13] Such different morphologies can have a strong influence on the macroscopic properties of the material such as ionic conductivities,[14] catalytic activities,[15] or luminescence.[16]

Structural changes in mechanically treated compounds can be studied by diffraction methods (e.g. X-ray or electron diffraction) combined with local structural methods like FT IR, Raman or solid state NMR spectroscopies.[17] The combination of these methods allows for investigating the relationship between the grinding time, particle size, and the different local environments of individual species present in the studied material.[18]

Here we investigate the consequences of the mechanical impact on samples with different chemical bonding situations resulting in different degrees of hardness (as a macroscopic quantity) using three ionic barium compounds: barium fluoride (BaF_2) as a typical representative for a soft fluoride compound, barium zirconate ($BaZrO_3$) as a typical representative for hard oxidic materials, and a layered compound barium chlorofluoride (BaFCl).

To investigate the influence of the grinding time on global and local structural changes depending on the crystal structure and hardness of the ground material, it is necessary to follow these changes with complementary methods. The changes in crystallinity of the samples upon grinding were investigated using powder X-ray diffraction (PXRD). Solid state NMR was used to probe the local environment of the metal atoms and its changes. Using this combination of methods, we were able to follow milling induced structural changes by powder X-ray diffraction including strain and crystallite size analysis. Changes

[a] Dr. S. Zänker, Dr. J. Marquardt, Dr. F. Emmerling
Department Materials Chemistry
Federal Institute for Materials Research and Testing (BAM),
Richard-Willstätter-Str. 11, D-12489 Berlin, Germany.
E-mail: franziska.emmerling@bam.de
[b] Dr. S. Zänker, Dr. G. Scholz, Dr. F. Emmerling
I Humboldt-Universität zu Berlin
Brook-Taylor-Str. 2, D-12489 Berlin, Germany

Supporting information for this article is available on the WWW under https://doi.org/10.1002/zaac.202200026

in the local structure were analyzed by ^{137}Ba solid state NMR, allowing to identify similarities and differences of milling induced changes in barium compounds of varying hardness.

Results and Discussion

The crystal structures and local environments of barium atoms for the three barium compounds are given in Figure 1. $BaZrO_3$ crystallizes in a cubic perovskite type structure (space group: *Pm*-3 *m*) where the Ba^{2+} is coordinated by twelve equivalent oxygen atoms to form BaO_{12} cuboctahedra (Figure 1a). $BaZrO_3$ is as a typical representative for hard oxide materials (Vickers hardness: $H_v = 4.95$ GPa).[19] BaF_2 crystalizes in the Fluorite type structure (space group: *Fm*-3 *m*) with a cubic coordinated Ba (Figure 1b). BaF_2 has a Vickers hardness of 0.9 GPa.[20] BaFCl crystallizes in the tetragonal space group *P4/nmm*. The Ba atoms are bonded in a nine-fold geometry to five equivalent Cl^- and four equivalent F^-ions (Figure 1c). The structure can be described as a layered structure with alternating F–Ba-Cl···Cl-Ba–F layers. The layers are connected by weak interlayer Cl···Cl interactions, which are weaker than ionic interactions between barium cations and fluorine or chlorine anions. These interactions of different strengths lead to an anisotropic behaviour of the hardness in BaFCl: the H_v on the (001) face is lower (0.63 GPa) then the H_v on (100) face (1.12 GPa).[21] In addition, this selection of samples addresses a further important point: BaF_2 and $BaZrO_3$ both crystallize in a cubic structure, in agreement with the structure the Vickers hardness is an isotropic parameter. In contrast, BaFCl crystallizes in a layered structure and the hardness experiences anisotropy.

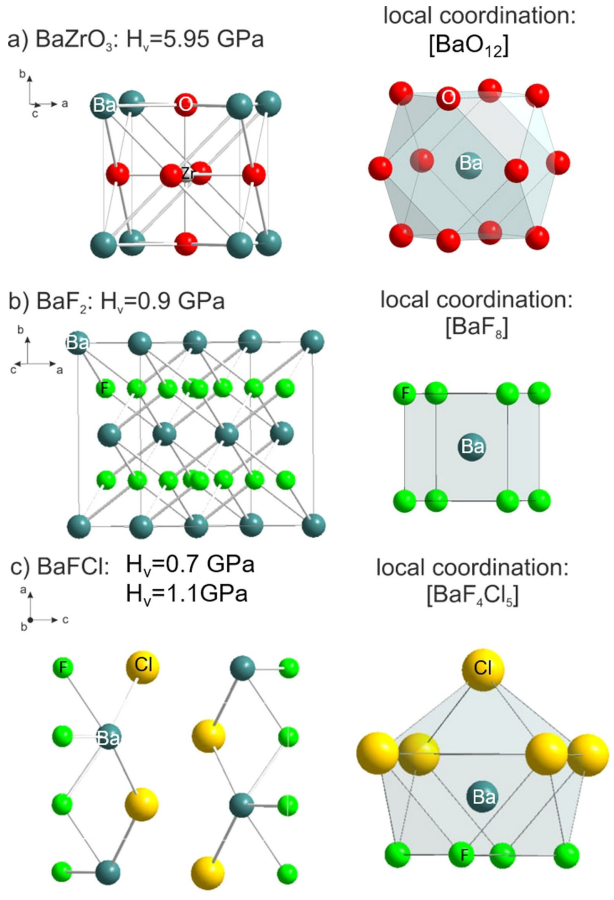

Figure 1. Details of crystal structures (left) and local environments of barium (right) of the studied materials along with their Vickers hardness (H_v): a) $BaZrO_3$ ($H_v = 5.95$ GPa), b) BaF_2 ($H_v = 0.9$ GPa), and c) BaFCl ($H_{v(001)} = 0.7$ GPa and $H_{v(100)} = 1.1$ GPa).

XRD

Figure 2 shows the X-ray diffractograms of the different Barium compounds before and after grinding. The detected reflections agree with those listed in the database.[22,23,24] Basically, an increase in grinding times leads to an increasing peak broadening (see section SII, Supporting Information). This is a typical effect which can be observed when the crystallite size is reduced and defects are incorporated into the crystal structure. To quantify changes in the crystalline content during the grinding process, a microstructure analysis was performed to determine the crystallite size and the deformation of the crystal lattice (strain). All refinements of microstructure analysis can be found in the SI (Section SII).

Figure 2a shows the X-ray diffractograms of barium zirconate ($BaZrO_3$) measured after different milling times. As mentioned above, barium zirconate ($BaZrO_3$) is the hardest of the materials studied here. In the X-ray diffractograms, only reflections of barium zirconate and silicon as internal standard (triangle: ▽) are visible. With increasing grinding time, the intensity of the reflections of the $BaZrO_3$ decreases. From the diffraction data, crystallite sizes and the deformations of the lattice were calculated via microstructure analysis.[25] After eight hours of milling, the average crystallite size was reduced by a factor of 3. The deformation of the crystal lattice increases with the grinding time indicating that the mechanical energy results in comminution and deformation of the lattice.

For barium fluoride (BaF_2) which is a significantly softer material than $BaZrO_3$ analogous effects of the milling process can be deduced from the diffractograms (s. Figure 2b). The crystallite size is reduced by a factor of 10 after eight hours of milling. Main grinding effects, however, are observed here in the first four hours of milling. Longer milling times lead to only marginal changes. These findings agree with determined sizes of the crystalline domains of other metal fluorides (CaF_2, AlF_3) for samples that were ground for longer than 4 hours.[26,27]

BaF_2 was also synthesized mechanochemically from barium hydroxide and ammonium fluoride (in Figure 2b, violet).[28,29] The mechanochemically synthesized sample shows that the crystalline regions are larger and more disturbed compared to BaF_2 that was ground for the same milling time. It can be assumed that during the mechanochemical formation of BaF_2 from $Ba(OH)_2$ and NH_4F small amounts of HF are formed locally which promotes crystallization, leading to a larger crystallite size.

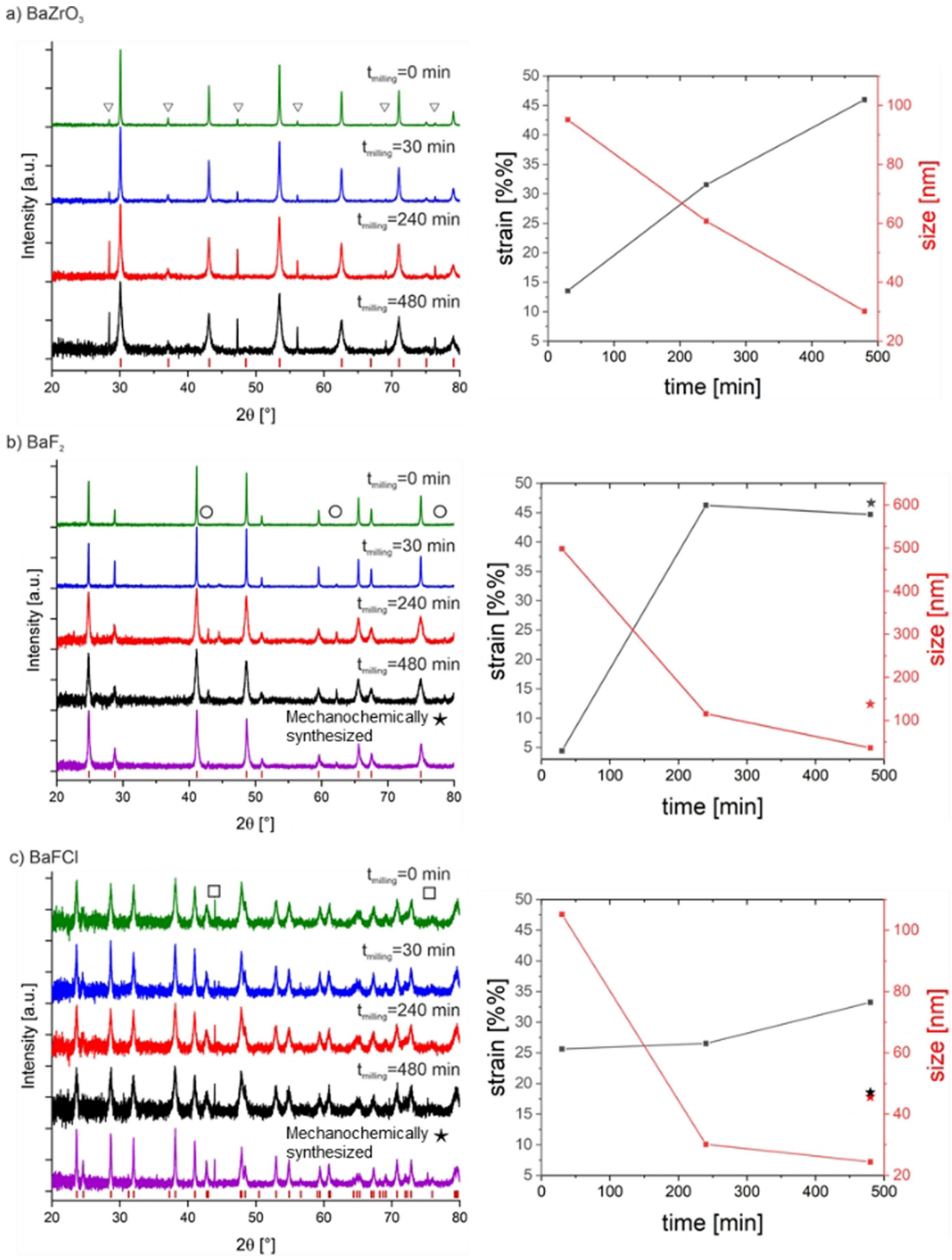

Figure 2. X-ray powder diffractograms of pristine and milled samples (left) together with the dependence of strain and crystallite size on milling time (right). The data are normalized to the intensity of the highest reflection. a) BaZrO3, b) BaF2, and c) BaFCl. The milling time is given directly in the figures. The violet diffractograms belong to mechanochemically synthesized samples with a milling time of 8 h. The crystallite sizes and strain for the mechanochemically synthesized samples are marked with asterisks (⋆) in the figures on the right side. For crystalline samples the positions of reflections according to the database is given with red bars below the diffractograms. (reflections of an internal standard: Si = ∇, MgO = ○, diamond = □).

The above mentioned effects for BaF_2 and $BaZrO_3$ have previously been reported for CaF_2,[27] α-AlF_3,[30] and for α-Al_2O_3.[26] In the case of milled corundum (α-Al_2O_3), it is assumed that the application of long milling times results in the presence of an amorphous protective layer around the crystalline region, which absorbs the mechanical energy and thus prevents further crushing and deformation.

The third studied compound, BaFCl, which has a comparable hardness to BaF_2, has a layered structure. Along these layers, the material can easily be separated, whereas perpendicular to the layers, the same material can only be split by a significantly greater impact. The intermolecular Cl···Cl bonds act as predetermined breaking points in the crystal structure. Effects of the grinding process can be seen in the X-ray diffractograms in Figure 2c similar to the other materials. The results of the microstructure analysis show that the crystalline regions can be reduced by a factor of 4. The reduction effect is somewhat similar to the effect observed for $BaZrO_3$. This is surprising, bearing in mind that for BaFCl the Vickers hardness is comparable to BaF_2, and not that of $BaZrO_3$. However, compared to the other materials, changes in the lattice deformation are significantly smaller. Most probably, the crystalline regions break up along the layers, rather than the crystal lattice being deformed due to the mechanical impact. The BaFCl, which was mechanochemically synthesized from BaF_2 and $BaCl_2$, has a larger average crystallite size and an even less deformed crystal lattice.

^{137}Ba NMR

The three compounds allow, in principle, ^{137}Ba solid state NMR experiments to be performed, which are quite scarce in the literature. Available literature on ^{137}Ba solid state NMR is mainly restricted to crystalline compounds which are of importance for ceramic materials[31,32,33] . Solid state ^{137}Ba NMR experiments[32] were already reported for crystalline $BaZrO_3$[33] which is also used as secondary standard in solid state NMR, and for crystalline BaFCl.[34] The influence of a milling impact on the local structures in $BaZrO_3$ and BaFCl as seen by ^{137}Ba NMR was not subject of previous studies. ^{137}Ba NMR spectra of crystalline and/or milled BaF_2 samples were not described in the literature to date.

The static ^{137}Ba NMR spectra of all studied crystalline compounds are given for a direct comparison in Figure 3. The high symmetric local environment of barium in BaF_2 and $BaZrO_3$ is reflected in the narrow signals at −0.57 ppm for BaF_2 (linewidth ~1.09 kHz) and at 279.3 ppm for $BaZrO_3$ (linewidth ~ 0.7 kHz). Whereas the signal of BaF_2 can be calculated with one single Lorentzian curve, the signal from $BaZrO_3$ requires two contributions: one contribution for the high symmetrically coordinated Ba^{2+} cations (single Lorentzian curve), and a second contribution implementing a distribution of quadrupolar parameters (Table 1, Figure SIII-3, Supporting Information). Obviously, there is also a certain degree of disorder or impurity already present in the crystalline starting material.

Due to the mixed fluorine/chlorine coordination of barium in BaFCl, the position of its barium signal can be expected between those of BaF_2 and $BaZrO_3$ and is found by simulation at 109.3 ppm in agreement with the literature.[34] The ^{137}Ba spectrum of crystalline BaFCl shows the typical line shape of a second order quadrupolar splitting, due to a mixed ligand coordination around barium. However, the resolution of the quadrupolar line shape is less ideal compared to the literature.[34] The synthesis conditions might be the reason for this circumstance. As possible consequence, we end up with a similar chemical shift and comparable quadrupolar frequency, but in addition we need the asymmetry parameter η_Q (s. Table 1) for the decomposition of the spectrum. The experimental and simulated ^{137}Ba spectrum of BaFCl is given in Figure SIII-2 (Supporting Information).

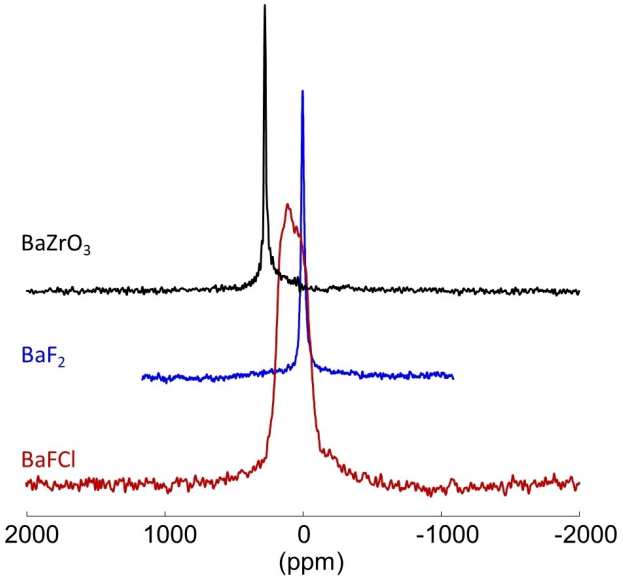

Figure 3. Static ^{137}Ba NMR spectra of crystalline BaF_2, BaFCl and $BaZrO_3$ samples.

Table 1. 137Ba NMR parameters obtained by simulation of the static spectra of pristine and milled Ba-samples.

Sample		δ_{iso} [ppm]*	$\nu_{Q\eta}$ [kHz]*	Ratio [%]
$BaZrO_3$	crystalline	279.3	–	57.8
		279.3	1127	42.2
	1 h milling	279.3	–	39.7
		279.3	1349	60.3
	8 h milling	279.3	–	18.2
		279.3	1797	81.8
BaF_2	crystalline	−0.57	–	100.0
	1 h milling	−0.57	–	50.2
		−0.57	1604	49.8
	8 h milling	−0.57	–	49.4
		−0.57	1617	50.6
	mechanochemical synthesis, 8 h	−0.57	–	71.1
		−0.57	1200	28.9
BaFCl	crystalline	109.3	832 (ν_Q)* 0.46 (η_Q)*	100.0

*δ_{iso}: value of the isotropic chemical shift; $\nu_{Q\eta}$: quadrupolar product; *ν_Q: quadrupolar frequency; *η_Q: asymmetry parameter of the quadrupolar interaction tensor.

All parameters obtained by simulation of the static spectra are summarized in Table 1. The influence of a milling impact on the ^{137}Ba spectra is presented for the three studied compounds in Figures 4, 5, and 6. Applying milling times up to four hours, the ^{137}Ba spectra of BaF_2 show a considerable effect on the spectral shape (Figure 4). Again, longer milling time (8 h) does not lead to any noticeable further changes, which is in agreement with results from PXRD and from the microstructure analysis for BaF_2. A decomposition of the spectra for the milled samples is not possible with only one single contribution. At least two contributions have to be taken into account: (i) one with a single Lorentzian curve for the still crystalline part, not or only little affected by the milling impact, and (ii) one applying the Czjzek-distribution function,[35] representing the increasing disorder in the grains on their surfaces by distribution of the quadrupolar parameters. As an example, the static ^{137}Ba NMR spectrum of 8 h milled BaF_2 is given in Figure SIII-1 (Supporting Information), along with its decomposition according to Table 1.

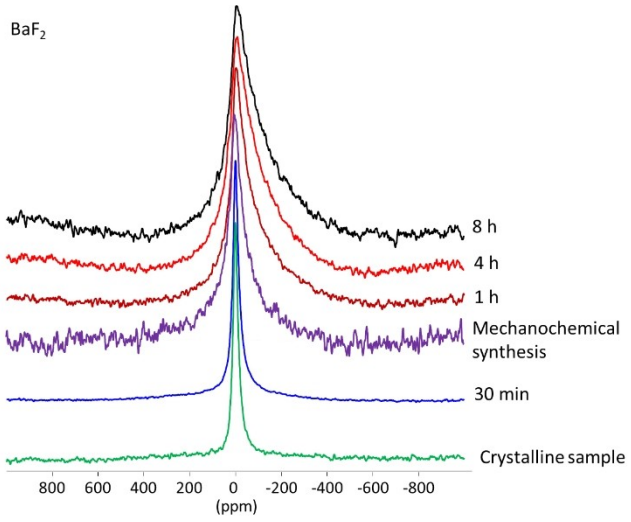

Figure 4. Static ^{137}Ba NMR spectra of milled and pristine BaF_2 samples. (Black, dark red, red: milling crystalline BaF_2; violett: mechanochemical synthesis from $Ba(OH)_2 + NH_4F$, 8 h in Si_3N_4 beakers).

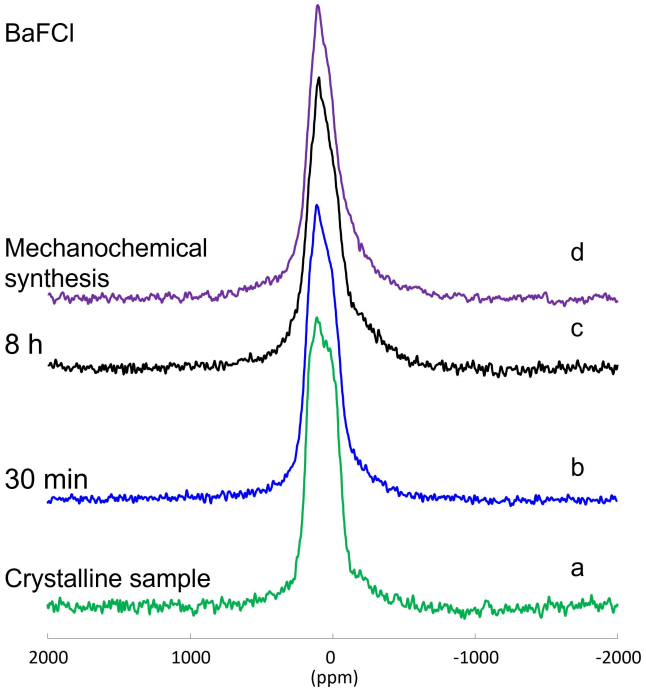

Figure 5. Static ^{137}Ba NMR spectra of milled and pristine BaFCl samples: a) Crystalline BaFCl, b) 30 min milling, c) 8 h milling, d) mechanochemical synthesis, 8 h.

As given in Table 1, the fraction of about 50% for each contribution of BaF_2 does not change remarkably in going from 1 h to 8 h of milling. This is in agreement with previous milling studies on CaF_2[27] and AlF_3[30] which showed that even smallest particles (2–5 nm) observed by TEM are crystalline. However, mechanochemically synthesized BaF_2 samples have a distinctly higher crystallinity and therewith a larger portion (71%) of the Lorentzian line, see Figure 4.

Following the very little changes in the ^{137}Ba spectral shape of BaFCl after grinding, it is almost impossible to perform a simulation of these spectra (Figure 5). This result is in agreement with findings of the microstructure analysis. For this compound an increase of lattice deformation and strain, which should have the main influence on the changes of the spectral shape of the ^{137}Ba NMR spectra, are neglectable. The very small changes in the ^{137}Ba NMR spectra support the theory that intermolecular Cl···Cl bonds act as a predetermined breaking point in the crystal structure.

For $BaZrO_3$ was found that the deformation of the crystal lattice increases proportionally to the grinding time (s. Figure 2a). These strong changes are unambiguously depicted in Figure 6. With increasing milling time, the portion of the narrow Lorentzian curve is decreased significantly from 57.8% for the crystalline starting material to only 18.2% for the 8 h milled sample. Accordingly, the portion of the second contribution including distributions of quadrupolar parameters increases from 42.2% to 81.8% after long time milling. Moreover, the quadrupolar product $\nu_{Q\eta}$ increases as well (see Table 1). Experimental and simulated ^{137}Ba NMR spectra are shown in Figure SIII-3 (Supporting Information). This strong growth of the second contribution obtained by application of the Czjzek-distribution function represents the increasing lattice deformation at milling.

The unknown origin of the second species with high degree of disorder present already in the crystalline $BaZrO_3$ (s. Table 1), which was used as starting material for milling, makes an unambiguous decomposition of the spectra almost impossible (cf. Figures 6 and SIII-3). However, it is distinctly visible that the portion of the narrow line, representing barium sites of high symmetry, decreases remarkably.

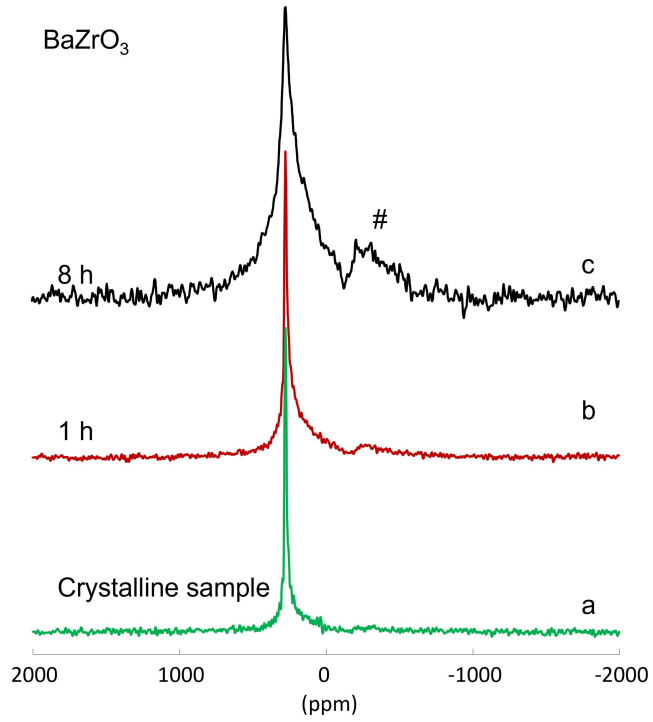

Figure 6. Static ^{137}Ba NMR spectra of milled and pristine $BaZrO_3$ samples: a) crystalline $BaZrO_3$, b) 1 h milling, c) 8 h milling.

Conclusions

Structural changes induced by mechanical milling of three barium compounds were followed by X-ray powder diffraction and ^{137}Ba solid state NMR, including a calculation of strain parameters and crystallite sizes, and a quantification of different contributions by decomposition of the solid state NMR spectra. The chosen materials $BaZrO_3$, BaF_2, and BaFCl show that grinding effects are governed by the close relation between crystal structure and hardness.

The consequences of the mechanical impact on global and local structures are not uniform as might be assumed in the first instance. They strongly depend on the internal chemical bonding situation of the substances, which manifests not only in different structures but also in different physical parameters such as hardness. Therefore, the consequences of a mechanical impact on different materials need to be discussed in relation to their chemical composition and their global and local structures. For all samples a decrease of crystallite sizes and an increase of the micro strain can be observed. The formation of disordered regions around the crystallites could be deduced by the decomposition of the ^{137}Ba solid state NMR spectra. The degree of such distortions, however, is quite different and depends on the chemical composition, structures, and hardness of the samples.

With the same milling time, these two compounds (BaF_2 and BaFCl) could also be produced mechanochemically. It was shown that the mechanochemical synthesis forms larger crystallites than the grinding of the target compounds from the storage bottle. The strain and the formation of disordered regions depend on the chemical bonding situation of the substances.

Comparing the behavior of the two cubic compound $BaZrO_3$ with BaF_2 grinding, shows that $BaZrO_3$ is much more affected by the mechanical impact. The latter can be followed both by PXRD and ^{127}Ba solid state NMR. On the other hand, BaF_2 and BaFCl possess comparable hardness but crystallize with different crystal structures. Even here the application of a milling impact leads to different results as a consequence of the layer structure of BaFCl.

In conclusion powder X-ray diffraction and solid state NMR are suitable complementary tools to follow global and local structural changes of powder samples at milling. A prediction of such changes always depends on a careful view on the bonding situations and cannot be generalized.

Experimental Section

Materials. $BaZrO_3$ and BaF_2 were purchased from Alfa Aesar (Purity 99%) and used without further purification. BaFCl was synthesized by dissolving $BaCl_2{\cdot}2H_2O$ (Roth, Purity 99%) in ethanol (Fluka, Purity 98%) and 1 eq. of ethanolic HF (Nanofluor GmbH, Purity 95%) was added. After 12 h the solvent was removed under reduced pressure allowing BaFCl to crystallize. The initial crystallite sizes of all samples were in the same order of magnitude.

Milling experiments.For milling, one gram of each starting material was ground for 30 min, 4 h, and 8 h in a planetary mill (Pulverisette 7 premium line, Fritsch, Germany). Zirconium oxide grinding bowls (volume: 45 mL) with five ZrO_2 balls (diameter: 10 mm, weight: 2.8 g) were used applying rotation speed of 600 rpm. The used ball to powder ratio was 14:1.

The mechanochemically synthesized BaF_2[28] or BaFCl[36] were prepared from $Ba(OH)_2$ and NH_4F or from $BaCl_2$ and BaF_2, respectively. One gram of the reactant mixtures was ground at 600 rpm for 8 hours.

XRD. Dependent on the studied material different internal standards (Si- (SRM 640d, National Institute of Standards & Technology), diamond powder (IDA Industrie-Diamant-Aachen), or MgO powder (EMSURE) powder) were added with a portion of 10% (see Table SII-1). This was necessary for an unambiguous discrimination between reflections of the respective sample and the standard. Powder diffraction measurements to determine the strain and crystallite size were performed on a D8 Discover diffractometer (Bruker AXS, Karlsruhe, Germany) operated in transmission geometry (Cu–Kα_1 radiation, $\lambda = 0.154056$ nm) and equipped with a Lynxeye detector. Samples were prepared in glass capillaries (diameter 0.5 mm) and measured over a 2θ-range between 20° and 85° with a step size of 0.006° and an acquisition time of 1.2 s per step. Microstructural analysis was performed using the FullProf Suite 3.0.0.[25,37] To account for instrumental effects, an instrumental resolution function based on a refinement of lanthanum hexaboride (LaB_6) was used. The background was interpolated between positions with no or low intensity contribution from peaks. The reflections in the diffractograms were fitted with pseudo-Voigt function.[38] Specifically, a Thompson-Cox-Hastings pseudo-Voigt convoluted with axial divergence asymmetry function was used.[39] First, the zero shift was determined by shifting the diffractogram until the reflections of the internal standards matched the hkl values of the phases (Si: COD 9011998;[40] diamond: ICSD 52054;[41] MgO: ICSD 9863[42]). The structure of the starting materials ($BaZrO_3$:

ICSD 97460;[22] BaF_2: ICSD 41649;[43] BaFCl: ICSD 2350[23]) and the corresponding structures of the internal standards were used as a starting model for the determination of the strain and the crystallite size. Subsequently, the parameters for the determination of the strain and the crystallite size were refined individually until reliable values for the parameters were found.

^{137}Ba solid state NMR. Both ^{135}Ba and ^{137}Ba are NMR active quadrupolar nuclei with a nuclear spin of $I = 3/2$. Due to its higher natural abundance (11.2%) and the higher gyromagnetic ratio ^{137}Ba is preferentially used as measured isotope. However, the large quadrupolar moment (24.5 fm^2) of ^{137}Ba has a strong effect of line broadening on the spectra. The only exception are Ba positions in high symmetric sites. For our measurements, a commercial $BaZrO_3$ sample of high crystallinity was taken as secondary standard for calibration, with the chemical shift of 279.3 ppm against zero of the 0.5 M $BaCl_2$ solution. The ^{137}Ba signal of $BaZrO_3$ showed a line width of only 140 Hz at a rotation frequency of 5 kHz.

All ^{137}Ba spectra were recorded using a 7 mm low-γ probe of Bruker-Biospin, operating at 9.4T ($\nu_L = 44.5$ MHz, Bruker Avance 400). All spectra shown in this contribution are static spectra recorded with a Hahn spin echo pulse sequence for static measurements. Dependent on the sample, the recycle delay was varied between 0.1 s and 10s, the number of accumulations between 50,000 and 230,000 scans and the spectral width between 100 kHz and 400 kHz. The shorter recycle delay and the larger number of scans was chosen for the mechanically milled samples. The simulation of the ^{137}Ba solid state NMR spectra was performed with the DMFIT program.[44]

Acknowledgements

Open Access funding enabled and organized by Projekt DEAL.

Conflict of Interest

The authors declare no conflict of interest.

Data Availability Statement

The data that support the findings of this study are available from the corresponding author upon reasonable request.

Keywords: mechanochemistry · X-ray diffraction · solid state NMR

[1] E. Boldyreva, *Chem. Soc. Rev.* **2013**, *42*, 7719–7738.
[2] S. L. James, C. J. Adams, C. Bolm, D. Braga, P. Collier, T. Friščić, F. Grepioni, K. D. Harris, G. Hyett, W. Jones, *Chem. Soc. Rev.* **2012**, *41*, 413–447; T. Friščić, C. Mottillo, H. M. Titi, *Angew. Chem. Int. Ed.* **2020**, *59*, 1018–1029; *Angew. Chem.* **2020**, *132*, 1030–1041; V. Boldyrev, K. Tkáčová, *J. Mater. Synth. Process.* **2000**, *8*, 121–132; A. A. Michalchuk, E. V. Boldyreva, A. M. Belenguer, F. Emmerling, V. V. Boldyrev, *Front. Chem.* **2021**, *9*, 359; C. Bolm, J. G. Hernández, *Angew. Chem. Int. Ed.* **2019**, *58*, 3285–3299; *Angew. Chem.* **2019**, *131*, 3320–3335.
[3] J. G. Hernandez, C. Bolm, *J. Org. Chem.* **2017**, *82*, 4007–4019.
[4] D. Crawford, J. Casaban, R. Haydon, N. Giri, T. McNally, S. L. James, *Chem* **2015**, *6*, 1645–1649; D. E. Crawford, C. K. Miskimmin, A. B. Albadarin, G. Walker, S. L. James, *Green Chem.* **2017**, *19*, 1507–1518; Q. Cao, J. L. Howard, D. E. Crawford, S. L. James, D. L. Browne, *Green Chem.* **2018**, *20*, 4443–4447.
[5] M. C. Lea, *Am. J. Sci.* **1894**, *47*, 377;P. Thießen, K. Meyer, G. Heinicke, *Grundlagen der Tribochemie, Abh. dtsch. Akad. Wiss.* **1966**; C. Suryanarayana, *Prog. Mater. Sci.* **2001**, *46*, 1–184; V. V. Boldyrev, *Russ. Chem. Rev.* **2006**, *75*, 177; P. Baláž, in *Mechanochemistry in nanoscience and minerals engineering*, Springer, **2008**, pp. 257–296.
[6] D. Braga, L. Maini, F. Grepioni, *Chem. Soc. Rev.* **2013**, *42*, 7638–7648.
[7] G.-W. Wang, *Chem. Soc. Rev.* **2013**, *42*, 7668–7700.
[8] C. Mottillo, T. Friščić, *Molecules* **2017**, *22*; D. Chen, J. Zhao, P. Zhang, S. Dai, *Polyhedron* **2019**, *162*, 59–64; M. Klimakow, P. Klobes, A. F. Thünemann, K. Rademann, F. Emmerling, *Chem. Mater.* **2010**, *22*, 5216–5221.
[9] V. Scalise, G. Scholz, E. Kemnitz, *J. Solid State Chem.* **2016**, *243*, 154–161; V. Scalise, G. Scholz, E. Kemnitz, *J. Mater. Sci.* **2018**, *53*, 13660–13668; G. Scholz, S. Brehme, M. Balski, R. König, E. Kemnitz, *Solid State Sci.* **2010**, *12*, 1500–1506; T. Friščić, C. Mottillo, H. M. Titi, *Angew. Chem.* **2020**, *132*, 1030–1041; *Angew. Chem. Int. Ed.* **2020**, *59*, 1018–1029.
[10] F. Gomollón-Bel, *Chem. Int.* **2019**, *41*, 12–17.
[11] a) P. Y. Butyagin, *Russ. Chem. Rev.* **1971**, *40*, 901; b) P.-A. Thiessen, K. Meyer, G. Heinicke, Berlin, Akademie-Verlag, Berlin, **1967**; c) P. Baláž, in *Mechanochemistry in Nanoscience and Minerals Engineering*, Springer, **2008**, pp. 297–405.
[12] V. Šepelák, A. Düvel, M. Wilkening, K.-D. Becker, P. Heitjans, *Chem. Soc. Rev.* **2013**, *42*, 7507–7520; P. Baláž, E. Godočíková, L. Kril'ová, P. Lobotka, E. Gock, *Mater. Sci. Eng. A* **2004**, *386*, 442–446; P. F. de Oliveira, R. M. Torresi, F. Emmerling, P. H. Camargo, *J. Mater. Chem. A* **2020**, *8*, 16114–16141.
[13] S. Zänker, G. Scholz, M. Heise, F. Emmerling, E. Kemnitz, *CrystEngComm* **2020**, *22*, 2772–2780.
[14] I. D. Gocheva, M. Nishijima, T. Doi, S. Okada, J.-I. Yamaki, T. Nishida, *J. Power Sources* **2009**, *187*, 247–252; F. Preishuber-Pflügl, M. Wilkening, *Dalton Trans.* **2016**, *45*, 8675–8687; M. Wilkening, A. Düvel, F. Preishuber-Pflügl, K. da Silva, S. Breuer, V. Šepelák, P. Heitjans, *Z. Kristallogr.* **2017**, *232*, 107–127.
[15] W. Oelerich, T. Klassen, R. Bormann, *J. Alloys Compd.* **2001**, *322*, L5–L9.
[16] M. Heise, G. Scholz, T. Krahl, E. Kemnitz, *Solid State Sci.* **2019**, *91*, 113–118; S. Zänker, G. Scholz, T. Krahl, C. Prinz, F. Emmerling, E. Kemnitz, *Solid State Sci.* **2021**, *117*, 106614.
[17] P. A. Julien, I. Malvestiti, T. Friščić, *Beilstein J. Org. Chem.* **2017**, *13*, 2160–2168; H. Kulla, S. Haferkamp, I. Akhmetova, M. Röllig, C. Maierhofer, K. Rademann, F. Emmerling, *Angew. Chem. Int. Ed.* **2018**, *57*, 5930–5933; *Angew. Chem.* **2018**, *130*, 6034–6038; S. Haferkamp, A. Paul, A. A. Michalchuk, F. Emmerling, *Beilstein J. Org. Chem.* **2019**, *15*, 1141–1148; M. Abdellatief, M. Abele, M. Leoni, P. Scardi, *J. Appl. Crystallogr.* **2013**, *46*, 1049–1057.
[18] V. Šepelák, I. Bergmann, S. Indris, A. Feldhoff, H. Hahn, K. D. Becker, C. P. Grey, P. Heitjans, *J. Mater. Chem.* **2011**, *21*, 8332–8337; V. Šepelák, S. Bégin-Colin, G. Le Caer, *Dalton Trans.* **2012**, *41*, 11927–11948; V. Šepelák, D. Baabe, D. Mienert, D. Schultze, F. Krumeich, F. Litterst, K. D. Becker, *J. Magn. Magn. Mater.* **2003**, *257*, 377–386; P. Druska, U. Steinike, V. Šepelák, *J. Solid State Chem.* **1999**, *146*, 13–21; V. Šepelák, I. Bergmann, A. Feldhoff, P. Heitjans, F. Krumeich, D. Menzel, F. J. Litterst, S. J. Campbell, K. D. Becker, *J. Phys. Chem. C* **2007**, *111*, 5026–5033; A. Düvel, E. Romanova, M. Sharifi, D. Freude, M. Wark, P. Heitjans, M. Wilkening, *J. Phys. Chem. C* **2011**, *115*, 22770–22780.

[19] S. Yamanaka, M. Fujikane, T. Hamaguchi, H. Muta, T. Oyama, T. Matsuda, S.-I. Kobayashi, K. Kurosaki, *J. Alloys Compd.* **2003**, *359*, 109–113.
[20] A. S. Reorrn, C. Stanford, *Am. Mineral.* **1974**, *59*, 885–888.
[21] J. Guille, M. Sieskind, *J. Mater. Sci.* **1991**, *26*, 899–903.
[22] I. Levin, T. G. Amos, S. M. Bell, L. Farber, T. A. Vanderah, R. S. Roth, B. H. Toby, *J. Solid State Chem.* **2003**, *175*, 170–181.
[23] M. Sauvage, *Acta Crystallogr. Sect. B* **1974**, *30*, 2786–2787.
[24] J. Leger, J. Haines, A. Atouf, O. Schulte, S. Hull, *Phys. Rev. B* **1995**, *52*, 13247.
[25] P. Scherrer, *Math. Phys. Appl. Math.* **1918**, *2*, 98–100.
[26] G. Scholz, R. Stösser, J. Klein, G. Silly, J. Buzaré, Y. Laligant, B. Ziemer, *J. Phys: Condens. Matter* **2002**, *14*, 2101–2117
[27] G. Scholz, I. Dörfel, D. Heidemann, M. Feist, R. Stösser, *J. Solid State Chem.* **2006**, *179*, 1119–1128.
[28] M. Dreger, G. Scholz, E. Kemnitz, *Solid State Sci.* **2012**, *14*, 528–534.
[29] G. Scholz, K. Meyer, A. Düvel, P. Heitjans, E. Kemnitz, *Z. Anorg. Allg. Chem.* **2013**, *639*, 960–966.
[30] G. Scholz, R. Konig, J. Petersen, B. Angelow, I. Dorfel, E. Kemnitz, *Chem. Mater.* **2008**, *20*, 5406–5413.
[31] a) Y. Liu, W. Zhang, B. Wang, L. Sun, F. Li, Z. Xue, G. Zhou, B. Liu, H. Nian, *Ceram. Int.* **2018**, *44*, 16475–16482; b) F. J. Loureiro, N. Nasani, G. S. Reddy, N. Munirathnam, D. P. Fagg, *J. Power Sources* **2019**, *438*, 226991; c) G. Taglieri, M. Tersigni, P. Villa, C. Mondelli, *Int. J. Inorg. Mater.* **1999**, *1*, 103–110; d) W. Shoulders, *Electronic Theses and Dissertations* **2013**, *2805*; e) N. Yedukondalu, K. R. Babu, C. Bheemalingam, D. J. Singh, G. Vaitheeswaran, V. Kanchana, *Phys. Rev. B* **2011**, *83*, 165117; f) A. Sutrisno, C. Lu, R. Lipson, Y. Huang, *J. Phys. Chem. C* **2009**, *113*, 21196–21201.
[32] K. MacKenzie, R. Meinhold, *Ceram. Int.* **2000**, *26*, 87–92.
[33] S. F. Dec, M. F. Davis, G. E. Maciel, C. E. Bronnimann, J. J. Fitzgerald, S. S. Han, *Inorg. Chem.* **1993**, *32*, 955–959.
[34] T. Bastow, S. Stuart, *Solid State Nucl. Magn. Reson.* **1996**, *6*, 95–100.
[35] J.-B. D. E. de Lacaillerie, C. Fretigny, D. Massiot, *J. Magn. Reson.* **2008**, *192*, 244–251.
[36] Z. Liu, M. A. Stevens-Kalceff, X. Wang, H. Riesen, *Chem. Phys. Lett.* **2013**, *588*, 193–197; X.-L. Wang, Z.-Q. Liu, M. A. Stevens-Kalceff, H. Riesen, *Inorg. Chem.* **2014**, *53*, 8839–8841.
[37] J. Rodríguez-Carvajal, *CEA/Saclay*, France **2001**.
[38] J. Rodríquez-Carvajal, T. Roisnel, in *Mater. Sci. Forum*, *Vol. 443*, Trans Tech Publ, **2004**, pp. 123–126.
[39] L. Finger, D. Cox, A. Jephcoat, *J. Appl. Crystallogr.* **1994**, *27*, 892–900.
[40] T. Hom, W. Kiszenik, B. Post, *J. Appl. Crystallogr.* **1975**, *8*, 457–458.
[41] T. Yamanaka, S. Morimoto, *Acta Crystallogr. Sect. B* **1996**, *52*, 232–238.
[42] S. Sasaki, K. Fujino, Y. Takéuchi, *Proc. Jpn. Acad. Ser. B* **1979**, *55*, 43–48.
[43] A. S. Radtke, G. E. Brown, *Am. Mineral.* **1974**, *59*, 885–888.
[44] D. Massiot, F. Fayon, M. Capron, I. King, S. Le Calvé, B. Alonso, J. O. Durand, B. Bujoli, Z. Gan, G. Hoatson, *Magn. Reson. Chem.* **2002**, *40*, 70–76.

Manuscript received: January 21, 2022
Revised manuscript received: March 25, 2022

RESEARCH ARTICLE

Changes in the global bulk and local structures, of three different barium compounds were induced by mechanical milling and followed using X-ray powder diffraction and solid state NMR spectroscopy.

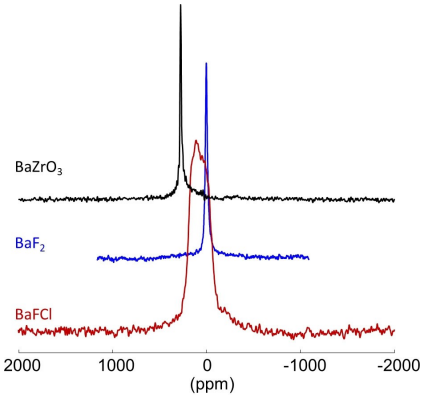

*Dr. S. Zänker, Dr. G. Scholz, Dr. J. Marquardt, Dr. F. Emmerling**